

Stabilization of a New Configurable Two-Wheeled Machine using a PD-PID and a Hybrid FL Control Strategies: A Comparative Study

M. Almeshal, M. O. Tokhi, K. M. Goher

Abstract—A novel design of two-wheeled robotic vehicle with moving payload is presented in this paper. A mathematical model describing the vehicle dynamics is derived and simulated in Matlab Simulink environment. Two control strategies were developed to stabilise the vehicle in the upright position. A robust Proportional-Integral-Derivative (PID) control strategy has been implemented and initially tested to measure the system performance, while the second control strategy is to use a hybrid fuzzy logic controller (FLC). The results are given on a comparative basis for the system performance in terms of disturbance rejection, control algorithms robustness as well as the control effort in terms of input torque.

Keywords—double inverted pendulum; modelling; robust control; simulation;

I. INTRODUCTION

MANY researchers have been interested in tackling the classical inverted pendulum (IP) control problem. These interests varied in between developing new configurations based on IP systems with multiple links and robotic applications such as [1][2][3][4], applying new control strategies [5][6][7], and applying optimization strategies to existing control scheme such as genetic algorithms and particle swarm optimization [8][9].

A novel configuration of two-wheeled double inverted pendulum-like balancing vehicle with a movable payload has been presented in [10]. A mathematical model derivation has been presented in [10] to describe system dynamics. The model will be used as a basis to test with different control schemes with different simulation scenarios. Two proposed control strategies are presented, a robust PID control and a hybrid FLC control strategy. This paper provides a comparison between the two control strategies in terms of robustness, rejection of external disturbances of various amplitudes and the control effort in terms of the input torques.

II. SYSTEM MATHEMATICAL MODEL

The vehicle configuration is presented in Fig. 1. The vehicle is designed based on the double inverted pendulum system model with novel modifications [1]. The vehicle consists of two links and a cart driven by two DC motors that in turn drive the entire system. In addition, the vehicle has a

third DC motor to drive the second link. These motors will help to stabilise the system in the upright position by applying an appropriate control signal. The second link consists of two co-axial rods connected by a linear actuator that enables lifting up the payload to a demanded height.

Therefore, the system has five degrees of freedom; translational motion with the right and left wheels, first and second links and linear actuator on the second link. The tilt angles of the first and second links are θ_1 and θ_2 respectively.

The linear displacement of the payload is defined as Q , while the angular displacements of the left and right wheels are defined as δ_L and δ_R respectively.

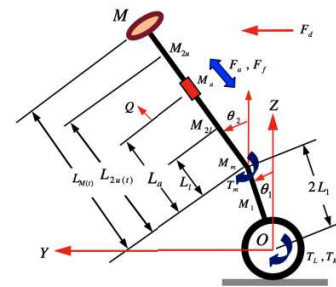


Fig. 1 Schematic description of the vehicle

The mathematical model of the system is presented by equations (1) to (5)

$$2C_{21}\ddot{\delta}_L + C_{22}\ddot{\delta}_R + C_9\frac{R_w}{2}L_1\ddot{\theta}_1\cos\theta_1 - C_9\frac{R_w}{2}L_1\dot{\theta}_1^2\sin\theta_1 + \frac{R_w}{2}(C_{10} + C_8Q)\ddot{\theta}_2\cos\theta_2 - \frac{R_w}{2}(C_{10} + C_8Q)\dot{\theta}_2^2\sin\theta_2 + \frac{R_w}{2}C_8\dot{Q}\dot{\theta}_2\cos\theta_2 = T_L - T_{Rl} \quad (1)$$

$$2C_{21}\ddot{\delta}_R + C_{22}\ddot{\delta}_L + C_9\frac{R_w}{2}L_1\ddot{\theta}_1\cos\theta_1 - C_9\frac{R_w}{2}L_1\dot{\theta}_1^2\sin\theta_1 + \frac{R_w}{2}(C_{10} + C_8Q)\ddot{\theta}_2\cos\theta_2 - \frac{R_w}{2}(C_{10} + C_8Q)\dot{\theta}_2^2\sin\theta_2 + \frac{R_w}{2}C_8\dot{Q}\dot{\theta}_2\cos\theta_2 = T_R - T_{Rr} \quad (2)$$

A. M. Almeshal and M. O. Tokhi are with University of Sheffield, United Kingdom (e-mail: a.m.almeshal@sheffield.ac.uk).

K. M. Goher is with Sultan Qaboos University, Oman (e-mail: kgoher@squ.edu.om).

$$\begin{aligned}
 & 2C_{18}\ddot{\theta}_1 + C_9 \frac{R_w}{2} L_1 (\ddot{\delta}_L + \ddot{\delta}_R) \cos \theta_1 - C_9 \frac{R_w}{2} L_1 (\dot{\delta}_L + \dot{\delta}_R) \dot{\theta}_1 \sin \theta_1 \\
 & + 2L_1 (C_{10} + C_8 Q) \ddot{\theta}_2 \cos(\theta_1 - \theta_2) - 2L_1 (C_{10} + C_8 Q) \dot{\theta}_1 \dot{\theta}_2 \sin(\theta_1 - \theta_2) \\
 & + 2L_1 (C_{10} + C_8 Q) \dot{\theta}_2^2 \sin(\theta_1 - \theta_2) + 2L_1 C_8 \dot{Q} \dot{\theta}_2 \cos(\theta_1 - \theta_2) \\
 & + C_9 \frac{R_w}{2} L_1 \theta_1^2 (\dot{\delta}_L + \dot{\delta}_R) \sin \theta_1 + 2L_1 (C_{10} + C_8 Q) \theta_1^2 \dot{\theta}_2 \sin(\theta_1 - \theta_2) \\
 & - C_3 g \dot{\theta}_1 \sin \theta_1 = \frac{1}{2} (T_{LT} + T_{RT})
 \end{aligned} \tag{3}$$

$$\begin{aligned}
 & C_{20} \ddot{\theta}_2 + (C_{12} \dot{Q} + 2C_8 Q) \dot{\theta}_2 + (C_{12} Q + C_8 Q^2) \ddot{\theta}_2 \\
 & + \frac{R_w}{2} (C_{10} + C_8 Q) (\ddot{\delta}_L + \ddot{\delta}_R) \cos \theta_2 \\
 & - \frac{R_w}{2} (C_{10} + C_8 Q) (\dot{\delta}_L + \dot{\delta}_R) \dot{\theta}_2 \sin(\theta_2) \\
 & + C_8 \frac{R_w}{2} \dot{Q} (\dot{\delta}_L + \dot{\delta}_R) \cos \theta_2 + 2L_1 (C_{10} + C_8 Q) \ddot{\theta}_1 \cos(\theta_1 - \theta_2) \\
 & - 2L_1 (C_{10} + C_8 Q) \dot{\theta}_1^2 \sin(\theta_1 - \theta_2) + 2L_1 (C_{10} + C_8 Q) \dot{\theta}_1 \dot{\theta}_2 \sin(\theta_1 - \theta_2) \\
 & + 2C_8 L_1 \dot{\theta}_1 \dot{\theta}_2 \cos(\theta_1 - \theta_2) + \frac{R_w}{2} (C_{10} + C_8 Q) (\dot{\delta}_L + \dot{\delta}_R) \dot{\theta}_2^2 \sin \theta_2 \\
 & - (C_{15} + C_8 Q) g \dot{\theta}_2 \sin \theta_2 \\
 & - 2L_1 (C_{10} + C_8 Q) \theta_1 \dot{\theta}_2^2 \sin(\theta_1 - \theta_2) = T_M - T_{FM} - L_d F_d \\
 & C_8 \ddot{Q} - \frac{1}{2} (C_{12} + 2C_8 Q) \dot{\theta}_2^2 - C_8 \frac{R_w}{2} \dot{\theta}_2 (\dot{\delta}_L + \dot{\delta}_R) \cos \theta_2 \\
 & - 2L_1 C_8 \dot{\theta}_1 \dot{\theta}_2 \cos(\theta_1 - \theta_2) + C_8 g \cos \theta_2 = F_a - F_{ja}
 \end{aligned} \tag{4}$$

$$\begin{aligned}
 & -2L_1 C_8 \dot{\theta}_1 \dot{\theta}_2 \cos(\theta_1 - \theta_2) + C_8 g \cos \theta_2 = F_a - F_{ja}
 \end{aligned} \tag{5}$$

III. CONTROL STRATEGIES

The strategy to control the system depends on developing a feedback control strategy of five control loops as shown in Fig.2. In order to drive the vehicle to undergo a specific planar motion in the XY plane, five feedback loops are developed. The angular position of the intermediate body is controlled by the measurement of the error in the position of link-1 and link-2. In order to control the position of the attached payload, a feedback control loop is developed with the error in the payload position as an input and the actuation force as the output of the control loop.

A. Robust PID Control Strategy

A combination of Proportional-Derivative (PD) and (PID) controllers were used to control the system. The PD controllers are used to control the two wheels angular displacement and the displacement of the payload actuator. While PID controllers are used to control the tilt angles of link-1 and link-2. A residual on the response over the required steady state level is obtained when implementing a PD controller on link-2. In order to compensate for this phenomenon, an integral part has been added in order to remove the steady-state error that appears in the response. Fig. 2 presents the Simulink block diagram of the controlled system.

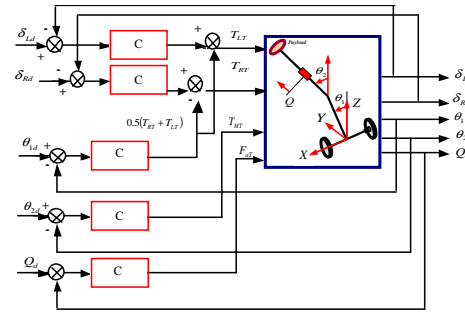


Fig. 2 Control strategy block diagram

B. Hybrid Fuzzy Logic Control Strategy

Two types of Hybrid FLC are designed and implemented to control the non-linear model of the two-wheeled vehicle. Proportional-Derivative-like fuzzy logic controller (PD-like FLC) is used to control the angular displacement of the wheels, the first link tilt angle and the payload linear actuator displacement. Where a PD plus integral fuzzy logic controllers (PD+I FLC) are used to control the links tilt angles to overcome the steady state error.

The inputs to the PD-like FLC are the error signal and the change of error. While the inputs for the PD+I FLC are the error signal, change of error and the sum of previous errors. The design of the FLC involves choosing a suitable fuzzy inference engine, defining the fuzzy rules and choosing the membership function type. At this stage of the research, the FLC presented is based on Mamdani-type of fuzzy inference engine with 25 fuzzy rule-base illustrated in Fig. 3. The generation of the fuzzy rules-base is based on the required system performance to minimize the system error between the output signal and the desired signal.

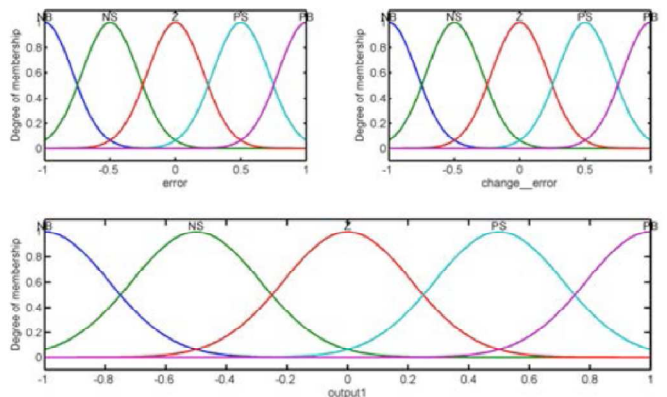


Fig. 3 Gaussian fuzzy membership functions

IV. SIMULATION RESULTS

A. Undisturbed Closed Loop System Response

Fig. 4 shows the system response with PID and FLC control strategies without any applied disturbance forces.

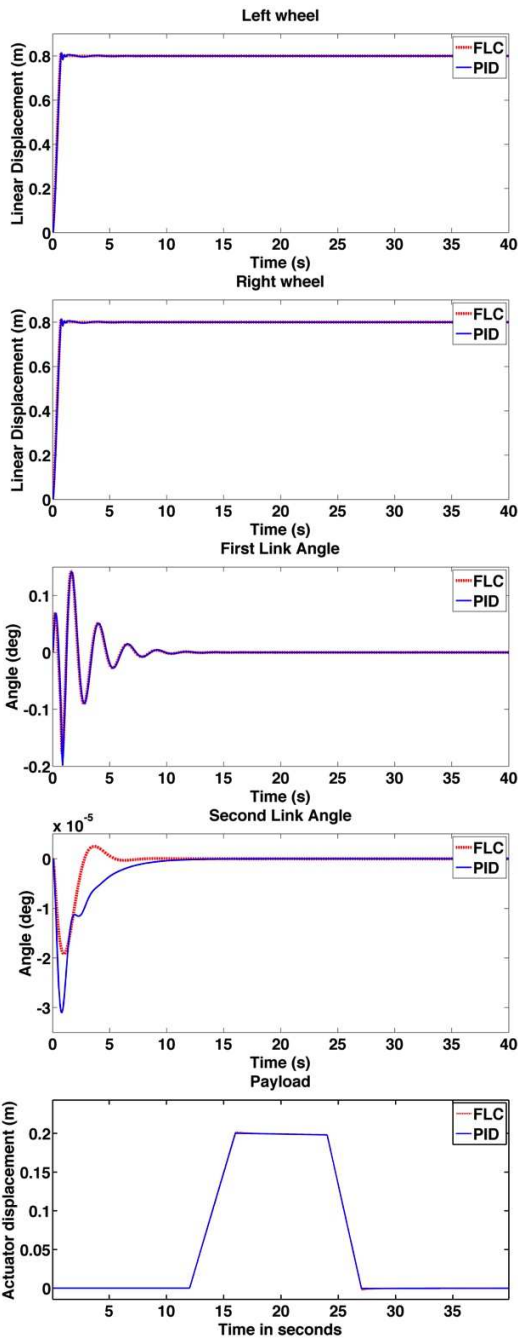


Fig. 4 PID/FLC controlled system response without disturbance forces

Fig. 5 presents the PID and FLC controller efforts in terms of the input torques.

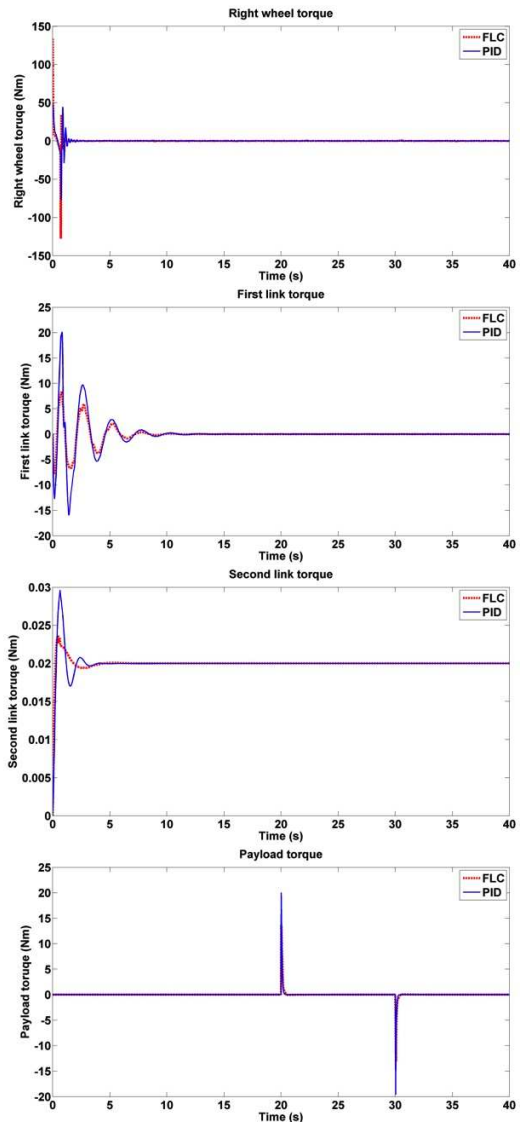
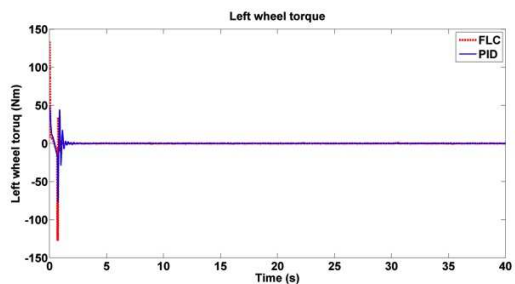


Fig. 5 PID/FLC controlled system response without disturbance forces

Referring to Figs 4 and 5, the FLC controller shows an improvement in the transient stage of the second link of the system. Moreover, a reduction in the input torque of the first link, second link and the payload linear actuator is noted.

B. External Disturbances With Various Amplitudes

Various disturbance amplitudes were applied to the system to evaluate the control robustness. In this paper, only a sample of these results is presented to suit the conference paper. The system response and control effort to an 80N disturbance force applied at the first link is presented in Figs 6 and 7 respectively.

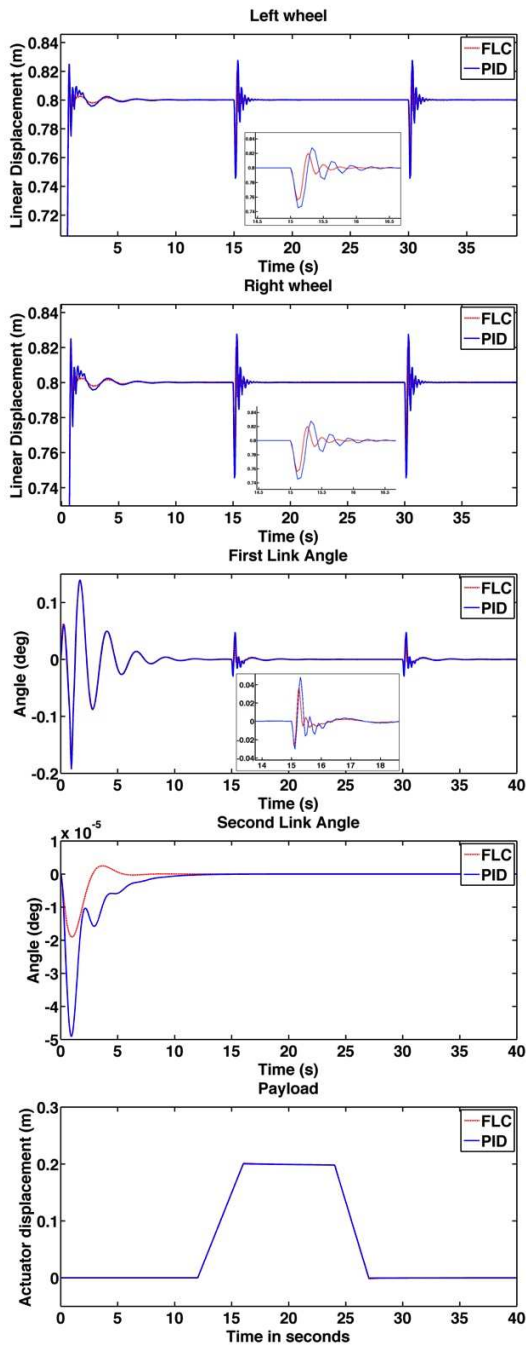


Fig. 6 PID/FLC controlled system response with 80 N disturbance force applied at the centre of the first link

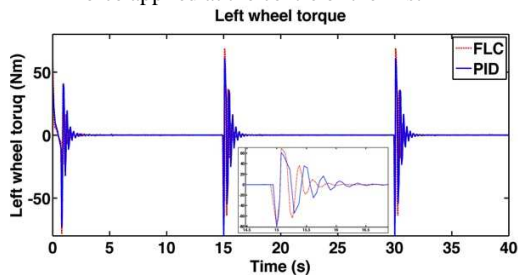


Fig. 7 PID/FLC Control efforts 80 N disturbance force applied at the centre of the first link

The FLC controller has rejected the disturbances a minimum overshoot and a least settling time than the PID controller. Comparing the controller efforts, the FLC controller have smaller overshoots at the first link, second link and the payload linear actuators.

While the FLC have slightly larger torque amplitude at the wheels, it successfully stabilised the cart with a smaller settling time than the PID controller.

Similarly, the disturbance force was applied at the centre of the second link. Figs 8 and 9 represent the response of the system and the control effort of the PID and FLC controllers respectively.

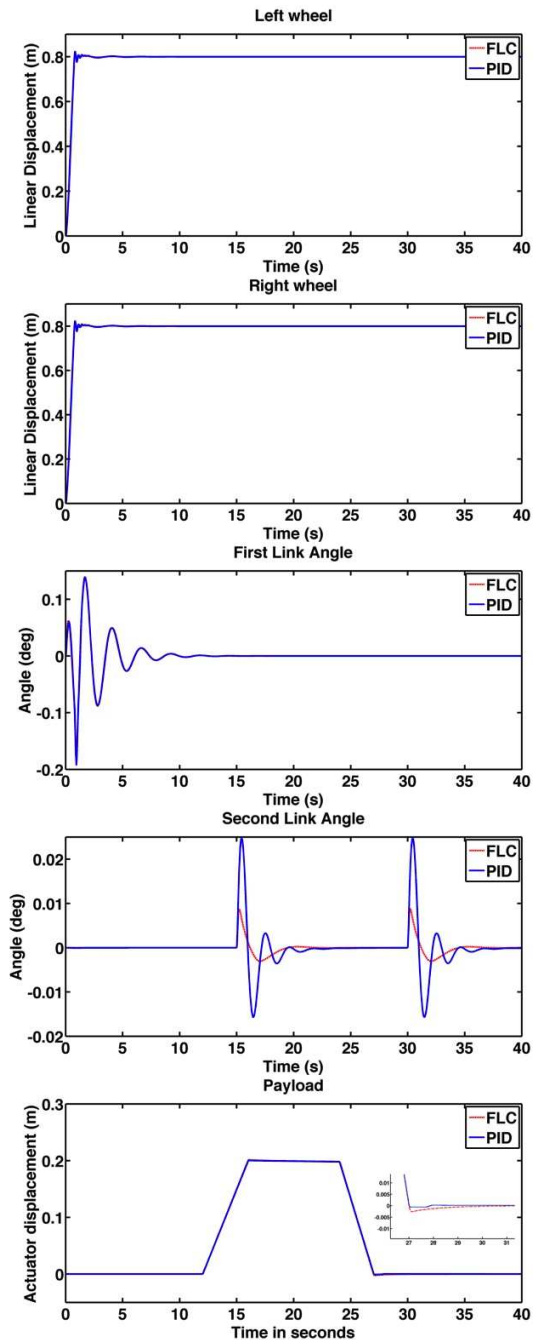


Fig. 8 PID/FLC controlled system response with 80 N disturbance force applied at the centre of the second link

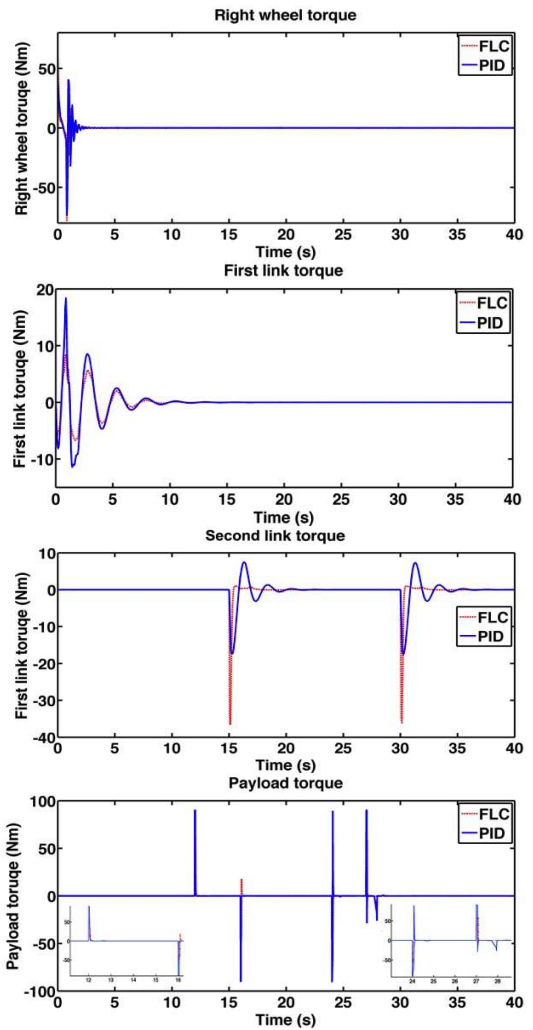
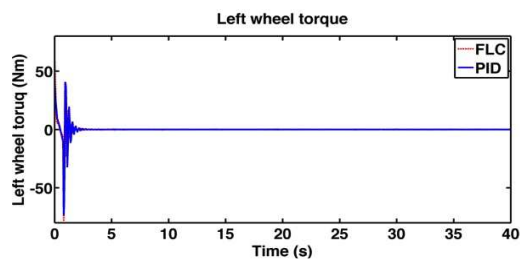
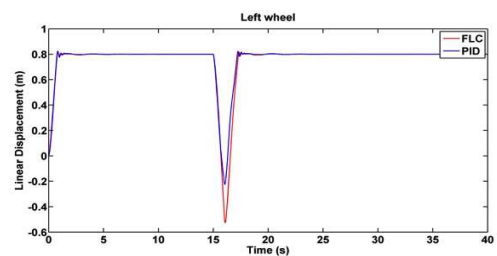


Fig. 9 PID/FLC Control efforts 80 N disturbance force applied at the centre of the second link

Clearly, the FLC have minimized the overshoot peak value at the second link in addition to a shorter settling time. At the displacement of the payload, the PID has resulted in some fluctuations appearing at the hard edges of the defined movement signal, while the FLC has a smoother transition with a negligible increase in the settling time but with a higher torque, due to the loop gain value, and a smaller control effort than the PID controller.

C. External Disturbances With Various Durations

Various durations of disturbances were applied to the system to evaluate the control robustness. A sample response to an 80N disturbance applied for 1 second is represented in Fig.10 and 11.



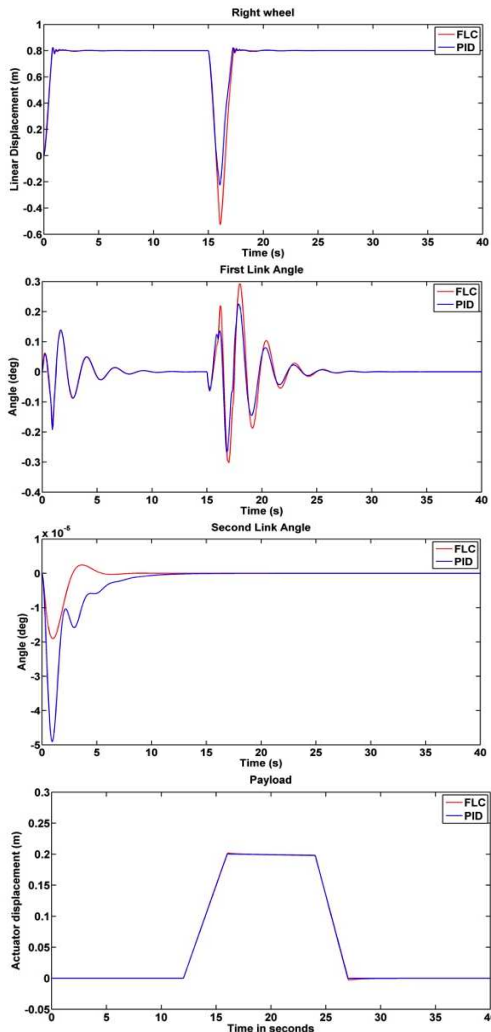


Fig. 10 PID/FLC controlled system response with disturbance applied for 1 second at the centre of the first link

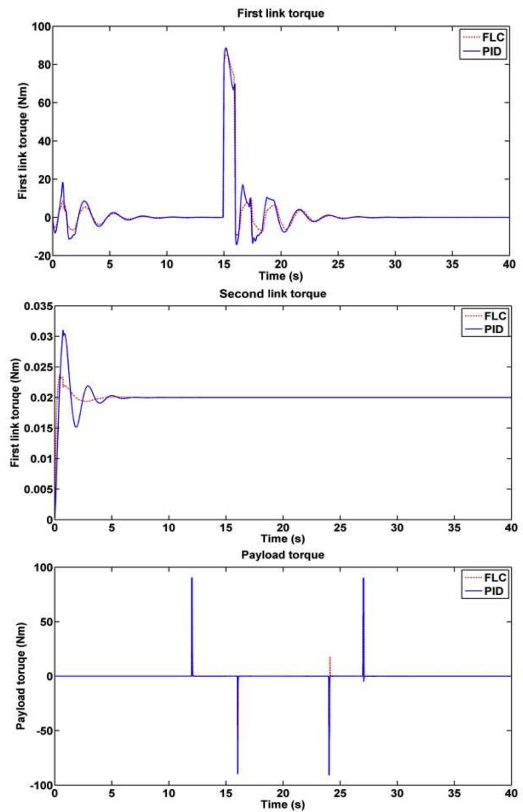
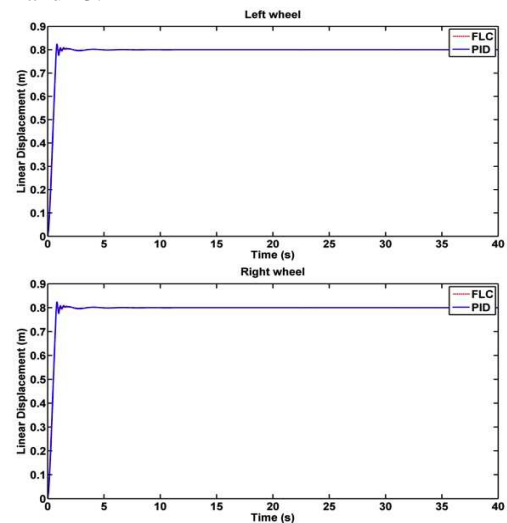
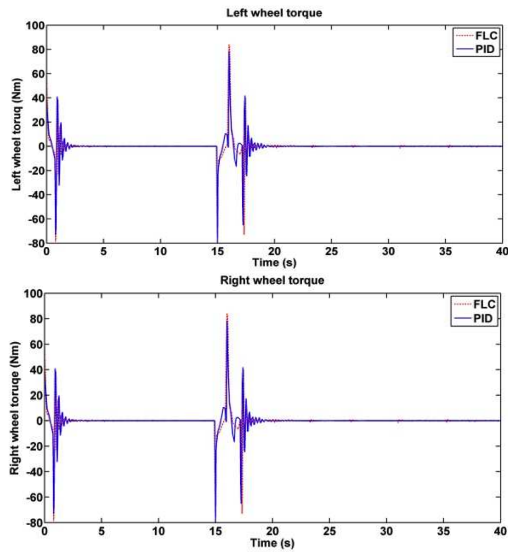


Fig. 11 PID/FLC Control efforts with disturbance applied for 1 second at the centre of the first link

Referring to Figs 10 and 11, the system had shown a better response with the PID than the FLC. The PID control has resulted in smaller overshoot with an exactly identical settling time of the FLC at the tilt angle of the first link. This is due to the high derivative gain of the PID controller.

Moreover, the PID has exerted a smaller torque value than the FLC controller to stabilise the system.

The disturbance with duration of 1 second was applied to the second link. The response of the system is presented in Figs 12 and 13.



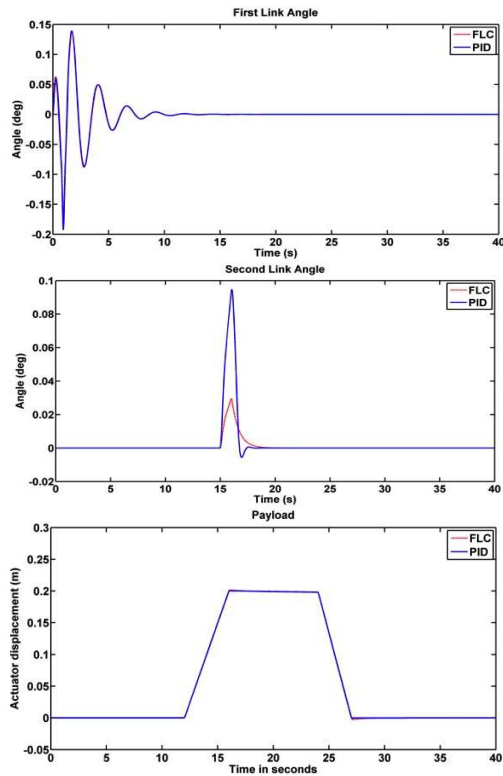


Fig. 12 PID/FLC controlled system response with disturbance applied for 1 second at the centre of the second link

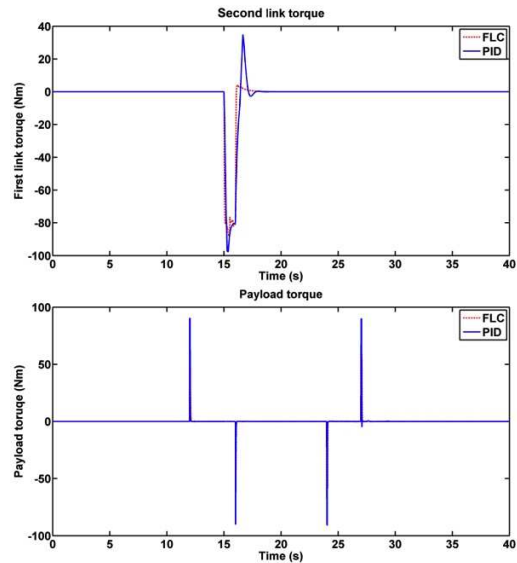


Fig. 13 PID/FLC Control efforts with disturbance applied for 1 second at the centre of the second link

On the contrary of the previous section, the FLC had a better control over the system than the PID controller. It can be noted that the overshoots were minimized, while maintaining an exact settling time with the PID controller. In addition, the FLC has exerted a smaller torque values compared to the PID controller.

V. CONCLUSIONS

A novel design of a two-wheeled vehicle has been presented. The vehicle system has been modelled using Lagrangian dynamic modeling.

Two control algorithms have been implemented on the system; PD-PID conventional control strategy and a hybrid FL control as indicated in details earlier.

The control parameters in this study were tuned heuristically to achieve a satisfactory performance and acceptable range of energy reduction. Disturbances have been applied on the system to test the robustness of both control strategies in terms of the ability to reject the disturbance effect. A disturbance force with a constant amplitude; 80 N has been applied on the vehicle components and the system response has been presented along with the control effort required.

Both control strategies have been able to stabilize the system under the effect of disturbance force. However, FLC strategy has showed much improvement, with/without external disturbance, in the transient period of oscillation of the second link as well as a significant reduction in the control effort. Both control approaches have shown somewhat an identical performance when dealing with the first link and the actuated payload.

REFERENCES

- [1] K. Goher, S. Ahmad, and O. M. Tokhi, "A new configuration of two wheeled vehicles: Towards a more workspace and motion flexibility," 2010 IEEE International Systems Conference, pp. 524-528, Apr. 2010.
- [2] Y. Takahashi and S. Ogawa, "Step climbing using power assist wheel chair robot with inverse pendulum control," Robotics and Automation, no. April, pp. 1360-1365, 2000.

- [3] S. Jeong and T. Takahashi, "Wheeled inverted pendulum type assistant robot: design concept and mobile control," *Intelligent Service Robotics*, vol. 1, no. 4, pp. 313-320, May 2008.
- [4] J. Zhao, "The control and design of Dual-wheel upright self-balance Robot," *Intelligent Control and Automation*, 2008. WCICA, pp. 4172-4177, 2008.
- [5] R. C. Tatikonda, V. P. Battula, and V. Kumar, "Control of inverted pendulum using adaptive neuro fuzzy inference structure (ANFIS)," *Proceedings of 2010 IEEE International Symposium on Circuits and Systems*, pp. 1348-1351, May 2010.
- [6] Z. Li and Y. Zhang, "Robust adaptive motion/force control for wheeled inverted pendulums," *Automatica*, vol. 46, no. 8, pp. 1346-1353, Aug. 2010.
- [7] M. Askari, H. a. F. Mohamed, M. Moghavvemi, and S. S. Yang, "Model predictive control of an inverted pendulum," *2009 International Conference for Technical Postgraduates (TECHPOS)*, pp. 1-4, Dec. 2009.
- [8] S. Ahmad, M. O. Tokhi, and S. F. Toha, "Genetic Algorithm Optimisation for Fuzzy Control of Wheelchair Lifting and Balancing," *2009 Third UKSim European Symposium on Computer Modeling and Simulation*, pp. 97-101, 2009.
- [9] X. Xiong and Z. Wan, "The simulation of double inverted pendulum control based on particle swarm optimization LQR algorithm," *2010 IEEE International Conference on Software Engineering and Service Sciences*, pp. 253-256, Jul. 2010.
- [10] A. Almeshal, K. Goher, and M. Tokhi, "Modelling of Two-Wheeled Robotic Wheelchair With Moving Payload," in *Proceedings of the 14th International Conference on Climbing and Walking Robots and the Support Technologies for Mobile Machines (CLAWAR 2011)*, 2011.